Atomic quantum corrals for Bose-Einstein condensates

Hongwei Xiong (熊宏伟)[1,2] and Biao Wu (吴飙)[2,3,4]

[1]*State Key Laboratory of Magnetic Resonance and Atomic and Molecular Physics, Wuhan Institute of Physics and Mathematics, Chinese Academy of Sciences, Wuhan 430071, China*

[2]*Kavli Institute for Theoretical Physics China, Chinese Academy of Sciences, Beijing 100190, China*

[3]*International Center for Quantum Materials, Peking University, Beijing 100871, China*

[4]*Institute of Physics, Chinese Academy of Sciences, Beijing 100190, China*

(Received 24 December 2008; revised manuscript received 9 June 2010; published 29 November 2010)

We consider the dynamics of Bose-Einstein condensates in a corral-like potential. Compared to the electronic quantum corrals, the atomic quantum corrals have the advantages of allowing direct and convenient observation of the wave dynamics, together with adjustable interaction strength. Our numerical study shows that these advantages not only allow exploration of the rich dynamical structures in the density distribution but also make the corrals useful in many other aspects. In particular, the corrals for atoms can be arranged into a stadium shape for the experimental visualization of quantum chaos, which has been elusive with electronic quantum corrals. The density correlation is used to describe quantitatively the dynamical quantum chaos. Furthermore, we find that the interatomic interaction can greatly enhance the dynamical quantum chaos, for example, inducing a chaotic behavior even in circle-shaped corrals.

DOI: 10.1103/PhysRevA.82.053634 PACS number(s): 03.75.Kk, 05.45.Mt, 67.85.De, 32.80.Qk

I. INTRODUCTION

Quantum corrals were first demonstrated by arranging iron adatoms into a ring on a copper surface [1,2]. Several years later, an optical analogy to the electronic quantum corrals was proposed theoretically and realized in experiment by a skillful arrangement of nanoscale pillars [3,4]. However, in both of the quantum corrals, only static wave properties were studied experimentally. Since the density image was obtained by sequential scanning over a period of time, the experimental study of wave dynamics in these corrals is difficult if not impossible.

In this paper, we study the dynamics of atomic quantum corrals for Bose-Einstein condensates (BECs). Since the density distribution of a BEC can be imaged snapshot by snapshot with a charge-coupled device (CCD), the atomic quantum corrals offer a great advantage over their electronic and optical counterparts, namely, the possible experimental study of the wave dynamics inside the corrals. Our numerical simulation shows that rich dynamical structures of a condensate can arise in the quantum corrals due to reflection and interference. Moreover, with a great deal of experimental control over the condensates [5,6], it is possible to study unique quantum behavior, which is unimaginable for electronic or optical quantum corrals. For example, the dynamic evolution of a quantized vortex confined inside quantum corrals can be studied.

Of particular importance, the atomic quantum corrals proposed here can be used as a laboratory to study quantum chaos. Since the first creation of quantum corrals, building stadium-shaped quantum corrals has been pursued to visualize experimentally the "scar" states, a signature of quantum chaos [7]. The stadium-shaped quantum corrals were built; however, the visualization of quantum chaos has remained elusive because the quantum corrals are too "leaky" for electrons [7]. Our atomic quantum corrals are very flexible and can be made to minimize the "leakage" so that they can be used to explore quantum chaos experimentally. As an example, we demonstrate with numerical simulation that with atomic quantum corrals of stadium shape, one should be able to visualize experimentally the quantum chaotic behavior predicted in Ref. [8]. We also show how the interference between two BECs is destroyed by chaos. In addition, our study finds that interaction can enhance quantum chaotic dynamics, inducing quantum chaos for circle-shaped quantum corrals.

The paper is organized as follows. In Sec. II, we consider the wave-packet dynamics for a BEC in a corral-like potential. In particular, the vortex evolution in a corral-like potential is studied. In Sec. III, we study dynamical quantum chaos for a BEC in stadium-shaped quantum corrals. In Sec. IV, the interaction effect on dynamical quantum chaos is studied. In particular, the density correlation is used to describe the interaction effect in the dynamical quantum chaos. A brief summary and discussion are given in the last section.

II. WAVE-PACKET DYNAMICS IN A CORRAL-LIKE POTENTIAL

We propose here a scheme to create quantum corrals for a BEC as illustrated in Fig. 1. An opaque sheet with a ring of holes is placed between a lens and a blue-detuned laser beam to create a corral-like repulsive potential for the condensate. The lens is to focus and adjust the sizes of the "corrals." The identical holes in the opaque sheet have a radius around 50 μm or larger, which is large enough so that the diffraction of the laser beam can be ignored. This setup is similar to the one used to create a rotating quasi-two-dimensional (quasi-2D) optical lattice by a mask with a set of holes [9] and a random potential [10] for BECs. One may also create this kind of quantum corral by using a spatial light modulator or microlens array [11].

We consider the situation that the condensate is tightly confined in the z direction so that the degree of freedom in the z direction is frozen out [12–16]. In this situation, we integrate out the axial degree of freedom and focus on the two-dimensional dynamics of the BEC, which is described by the following Gross-Pitaevskii (GP) equation [12]:

$$i\frac{\partial\Phi}{\partial t} = -\left(\frac{\partial^2}{\partial x^2}+\frac{\partial^2}{\partial y^2}\right)\Phi + V_{\rm oc}\Phi + V_{\rm ht}\Phi + g_{\rm 2D}|\Phi|^2\Phi\,, \tag{1}$$

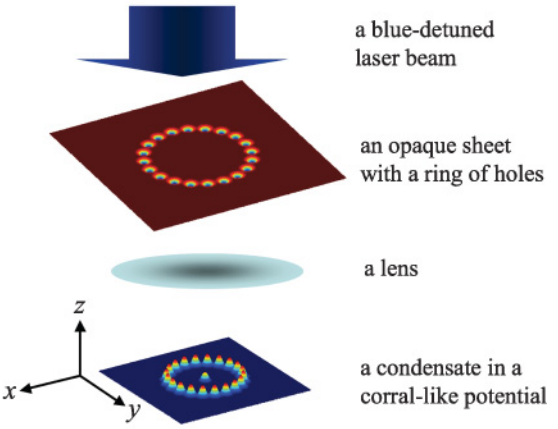

FIG. 1. (Color online) Scheme to build quantum corrals for a Bose-Einstein condensate (see text).

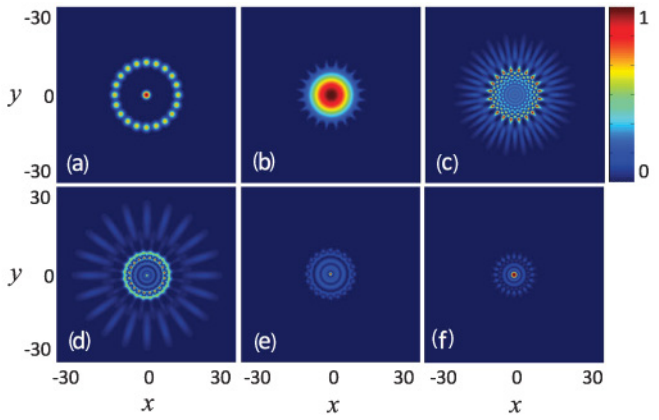

FIG. 2. (Color online) Density distribution of a condensate in a corral-like potential at different times: (a) $t = 0$, (b) $t = 1$, (c) $t = 2$, (d) $t = 3$, (e) $t = 4$, and (f) $t = 5$. The coordinates are in units of L_0. In (a), the corral-like potential is shown.

where Φ is a normalized wave function. This equation has been made dimensionless with the length unit L_0 and the energy unit $E_0 = \hbar^2/2mL_0^2$. The time unit is then $T_0 = \hbar/E_0$. $V_{\rm oc}$ is the corral-like potential, and $V_{\rm ht} = m\omega_\perp^2 L_0^2(x^2 + y^2)/2E_0$, with $\omega_\perp$ being the harmonic frequency in the x and y directions. In the numerical calculations, we choose m as the mass of the sodium atom and use $L_0 = 5\ \mu$m, which means $T_0 = 18.3$ ms.

The ith Gaussian potential $V_i(x,y,z)$ created by a focused laser beam propagating along the z direction has the following form:

$$V_i(x,y,z) \sim \frac{P}{\pi\sigma^2(z)} e^{-[(x-x_i)^2+(y-y_i)^2]/\sigma^2(z)}, \tag{2}$$

where P is the total power of a laser beam and

$$\sigma(z) = \sigma_0\sqrt{1 + z^2/z_R^2}, \tag{3}$$

with the Rayleigh length $z_R = 2\pi\sigma_0^2/\lambda$. In the following calculations, $\sigma_0 = 5\ \mu$m. For a focused laser beam with wavelength $\lambda = 500$ nm, we have $z_R = 314\ \mu$m. In this situation, along the z direction, the condensate feels almost the same corral-like potential in the x-y plane.

To show clearly the fundamental properties of the atomic quantum corrals, we calculate numerically the evolution of the condensate confined in circle-shaped quantum corrals,

$$V_{\rm oc} = \sum_{j=1}^{M} \gamma e^{-[(x-x_j)^2+(y-y_j)^2]/\sigma^2}, \tag{4}$$

with $\{x_j, y_j\}$ distributed uniformly along a circle of radius R. In our calculation, the parameters are $\gamma = 20$, $M = 20$, $R = 10$, $\sigma = 1$, $g_{2D} = 50$, and $\omega_\perp = 70 \times 2\pi$. We first get the ground-state wave function by using the widely used imaginary time propagation (ITP) method. Then the evolution of the condensate after the harmonic trap is suddenly switched off is followed numerically with the GP equation (1). In Fig. 2(a), both the initial density distribution $|\Phi|^2$ and the corral-like potential are shown. Illustrated in Figs. 2(b)–2(f) is the evolution of $|\Phi|^2$ after the sudden switching off of the harmonic trap. The rich and colorful structures in $|\Phi|^2$ originate from the following two physical mechanisms:

(i) After switching off the harmonic trap and with the expansion of the condensate, the condensate will be reflected by the corral-like potential. The expanding and reflected condensates will overlap and lead to clear interference patterns. In Figs. 2(c)–2(f), a series of ring-shaped interference fringes are clearly shown.

(ii) In Figs. 2(c) and 2(d), the density distribution shows sunflower-like structure. This sunflower-like structure is due to the discrete characteristic of the corral-like potential. For the expanding condensate, the corral-like potential can be regarded as discrete scattering sources arranged along a circle. This discrete characteristic imposes important modulation on the interference fringes. As a result, the ring-shaped interference fringe develops a series of small peaks. In Figs. 2(c) and 2(d), the number of small peaks distributed along an interference fringe is found to be exactly 20, the number of corrals.

For the parameters of Fig. 2, the interaction plays a negligible role because just before the collision between the condensate and the quantum corrals, most of the interaction energy has already transformed into kinetic energy: Just before the collision between the condensate and the corrals, the size of the condensate is about 50 times larger than the initial size. In this work, except for the parameters used in Sec. IV, where the interaction effect will be stressed, the interaction effect will not play a dominant role in the dynamic process of the condensate.

We now consider the evolution of a quantized vortex in the circle-shaped quantum corrals. In our calculations, we use $\gamma = 20$, $M = 20$, $R = 10$, $\sigma = 1$, $g_{2D} = 50$, and $\omega_\perp = 70 \times 2\pi$. The initial vortex state in the presence of both the corral-like and harmonic trapping potentials is obtained numerically from the ITP method with a trial wave function, which has the general form $f(\sqrt{x^2 + y^2})e^{\pm i\theta}$ [6]. The plus and minus signs in $e^{\pm i\theta}$ denote the rotational directions of the vortex.

The evolution of the vortex in the corrals after the harmonic trap is switched off is shown in Fig. 3. The evolution is obtained numerically from the GP equation (1). Similarly, the expanding and reflected condensates will overlap and lead to clear interference patterns. These interference patterns are clearly seen in Figs. 3(a)–3(f), where Figs. 3(a)–3(c) show the evolution for the case of $e^{i\theta}$ and Figs. 3(d)–3(f) give the evolution for the case of $e^{-i\theta}$.

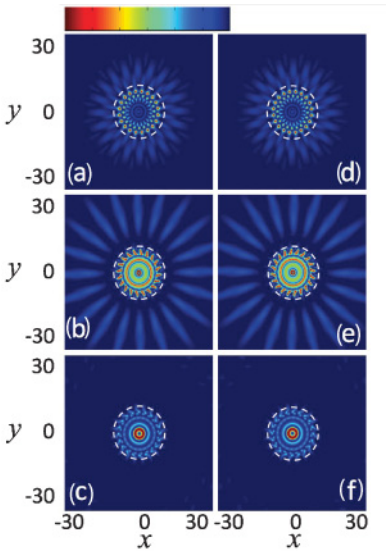

FIG. 3. (Color online) Density distributions of a quantized vortex in a corral-like potential at different times. The left column shows a vortex rotating counterclockwise at (a) $t = 2.5$, (b) $t = 3.8$, and (c) $t = 6.3$. The right column shows a vortex rotating clockwise at (d) $t = 2.5$, (e) $t = 3.8$, and (f) $t = 6.3$. The coordinates are in units of L_0. The dashed circles mark the position of the circular corrals.

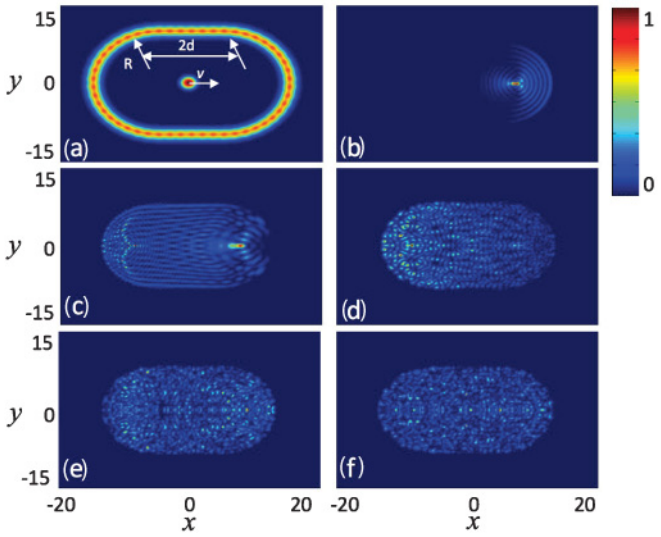

FIG. 4. (Color online) Density distributions of a condensate in a stadium-shaped potential at different times: (a) $t = 0$, (b) $t = 0.5$, (c) $t = 1$, (d) $t = 1.5$, (e) $t = 3$, and (f) $t = 6$. Here the time t is in units of $T_s = 2(R + d)/v$, which is the time needed for a classical particle to propagate along the stadium axis. The coordinates are in units of L_0. In (a), the stadium-shaped confinement potential is also shown.

In addition to the sunflower-like structure induced by the discrete characteristic of the corral-like potential, one more interesting feature has emerged due to the presence of the vortex. At $t = 2.5T_0$, as shown in Figs. 3(a) and 3(d), the two different vortices have almost identical density distributions even though their sunflower-like structure indicates that the two BECs have already felt the corral potential. The rotational difference between the two BECs shows up only when the "main peak" of the condensate hits the corral potential, as shown in Figs. 3(b) and 3(c) and 3(e) and 3(f). This is due to the unique property of the velocity field for a quantized vortex, where the center of the vortex has larger velocity. In Figs. 3(c) and 3(f), a series of flyerlike peaks distributed along the circumference of the outmost circle distinguishes obviously two vortices with different rotational directions. This feature may be applied to detect the rotational direction of a vortex.

It is still an open problem to experimentally investigate the behavior of a quantized vortex in electronic quantum corrals. For an atomic condensate, all the rich dynamics of the vortex shown here can be readily observed experimentally because a vortex in a BEC can be generated with mature technologies [17]

III. QUANTUM CHAOS FOR A BEC IN A CORRAL-LIKE POTENTIAL

We now turn to consider the dynamics of a BEC confined in stadium-shaped quantum corrals, as shown in Fig. 4(a). The stadium billiard is a typical system used to study both classical and quantum chaos [8]. The energy-level distribution was proposed in Ref. [18] to reveal the quantum chaos for a BEC. The discrete chaotic state, chaotic shock wave, and soliton-chaos transition were studied recently [19]. Most recently, the scars in the steady-state density profiles of parametrically driven condensates were proposed to study quantum chaos [20].

There was a series of pioneering experiments exploring chaos with cold atoms [21–24]. However, most of these experiments, in particular, the ones with optical billiards [22–24], were focused on classical chaos. For example, in Ref. [23], a classic chaotic motion was observed with a stadium billiard having a hole by observing a fast and purely exponential decay for the fraction of surviving atoms.

Here we focus on the dynamic manifestation of quantum chaos with a BEC. The stadium potential can be described by V_{oc} with $\{x_i, y_i\}$ uniformly distributing along the circumference of the stadium, as shown in Fig. 4(a). In our numerical computation, the parameters that we choose for the stadium-shaped quantum corrals are $M = 50, \sigma = 1, \gamma = 500, R = 10, g_{2D} = 50$, and $d = 30\pi/19$. The ground-state wave function is calculated for the condensate confined in the harmonic trap with $\omega_\perp = 87.5\pi$ and the stadium-shaped quantum corrals. This condensate is then given an initial velocity of v. After switching off the harmonic trap, we study numerically the evolution of this moving condensate in the stadium-shaped quantum corrals. For $v = 2.7$ mm/s, Figs. 4(a)–4(f) show a series of snapshots for the condensate evolution. The regular density distribution is destroyed after a small number of reflections. This is in stark contrast to the dynamics of a moving BEC in circle-shaped quantum corrals, which stays regular even after long-time evolution, as indicated by the clear interference patterns in Fig. 5. This significant difference can be used in an experiment to identify the dynamical quantum chaos for stadium-shaped quantum corrals. The parameters for Fig. 5 are $M = 40$, $\sigma = 1$, $\gamma = 500$, $R = 10$, $\omega_\perp = 87.5\pi$, $g_{2D} = 50$, and $v = 2.7$ mm/s.

This quantum chaotic behavior was first revealed in Ref. [8] for a free particle in a continuous stadium billiard. In their

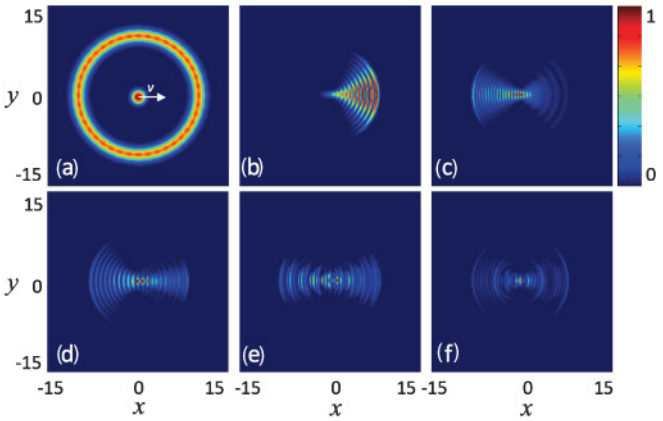

FIG. 5. (Color online) Density distributions of a condensate in a circle-shaped potential at different times: (a) $t = 0$, (b) $t = 0.5$, (c) $t = 1$, (d) $t = 1.5$, (e) $t = 3$, and (f) $t = 6$. Here the time t is in units of $T_c = 2R/v$. The coordinates are in units of L_0. In (a), the circle-shaped confinement potential is also shown.

work, Tomsovic and Heller showed that the chaotic wave dynamics shown in Fig. 4 can be regarded as the supposition of millions of classical trajectories. The random-looking sequence in Fig. 4 is just a reflection of the chaotic classical trajectories.

As mentioned, it has remained elusive to visualize experimentally the quantum chaotic behavior in the electronic quantum corrals despite a great deal of effort [7]. The main reason is that the quantum corrals are too leaky for electrons. Our numerical studies here show that the BEC system provides a very good chance to experimentally visualize the quantum chaos because (i) the stadium-shaped corrals can be built with the scheme shown in Fig. 1 and 2 the BEC can gain a velocity with the method used for the experimental studies of quantum reflection [25]. As the length unit is 5 μm in Figs. 2–5, an imaging resolution below 5 μm is necessary to reveal the structure in these figures. Fortunately, absorption imaging with resolution lower than 5 μm has been achieved [26]. Classical chaotic behavior has been studied experimentally with nondegenerate cold atomic gases [22–24]. Quantum chaos has been visualized with classical wave systems, such as sound and microwave [27]. An eventual implementation of our scheme will be an experimental realization of quantum chaos with a coherent matter wave, marking an important step forward in the experimental studies of chaos.

When comparing our results to the microwave systems [27,28], we see that the propagation of the microwave under the stadium boundary condition renders less-complex scar distribution. This obvious difference between microwave and atomic condensate originates from different dispersive relations. The dispersive relation of a microwave is $\varepsilon_p = pc$, whereas it is $\varepsilon_p = p^2/2m$ for an atomic wave packet. These different dispersive relations imply that there is no wave-packet diffusion for a microwave in free space, while there is diffusion for an atomic wave packet. This diffusion effect of the atom makes the interference phenomenon more complex and thus leads to more-complex scar distribution.

Besides visualizing the known quantum chaotic behavior, we can explore more on quantum chaos with BECs in

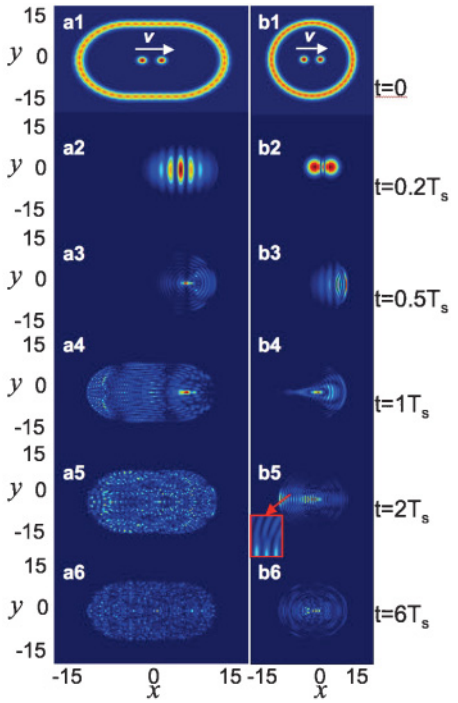

FIG. 6. (Color online) The evolution of two initially coherently separated condensates in stadium-shaped (left column) and circle-shaped potentials (right column). Each figure in the left and right columns is 30×40 and 30×30, with coordinate units of L_0, respectively. Here the time unit is $T_s = 2(R + d)/v$ and $T_c = 2R/v$ for the left and right columns, respectively.

stadium-shaped corrals. It is well known that the interference between two condensates can show the phase coherence of the condensates [29]. It is therefore interesting to see how quantum chaos would affect the interference. For this purpose, we study two coherently separated BECs in stadium-shaped corrals. Another significance of this study lies in that a classical particle can never be regarded as two coherently separated particles. We show in Fig. 6 the evolution of two initially coherently separated condensates [29] for both stadium-shaped and circle-shaped corrals. Figures 6(a1)–6(a6) give the evolution of two coherently separated Gaussian wave packets with the same boundary condition in Fig. 4. The initial width and distance are $\sqrt{2/5}$ and 4, respectively. For short-time evolution, the interference between two condensates is seen in Fig. 6(a2). After long-time evolution, the interference is destroyed by quantum chaos, as seen in Figs. 6(a4)–6(a6). As a comparison, we have also computed the evolution of these two BECs in circle-shaped corrals. The results are shown in Figs. 6(b1)–(b6), where the interference between two condensates is partly preserved, even for long-time evolution. In the inset of Fig. 6(b5), the forklike structure implies the information of two initially coherently separated condensates. These results demonstrate that quantum chaos can cause the loss of phase memory (or the breakdown of the phase coherence) between two condensates.

For the parameters in the numerical calculations in this section, most of the interaction energy has been transferred into kinetic energy. In this situation, we expect the quadrupole mode would not play an important role. In addition, the

stadium-shaped quantum corrals are symmetric about the x axis and y axis, which will lead to a suppression of the quadrupole mode.

IV. THE ROLE OF INTERATOMIC INTERACTIONS ON THE DYNAMICAL QUANTUM CHAOS

An important advantage of a BEC in dilute gases is that the coupling constant can be controlled with Feshbach resonance [30] or by manipulating the trapping frequency perpendicular to the quantum corrals [12]. Compared with the microwave experiment in stadium-shaped quantum corrals [27], the controllability of the coupling constant for degenerate quantum gases gives us a chance to consider also the role of interatomic interactions on dynamical quantum chaos.

The effect of atomic collisions for thermal atoms in optical billiards has been discussed by Milner *et al* [22], who described well the results using the classical picture. For a BEC, the interaction is well described by the nonlinear term in the GP equation. This makes it possible to reveal and quantify the interaction effect on quantum chaos

To reveal the role of interatomic interactions on the quantum chaos, we consider a density correlation function defined as

$$C_n = \int n(t=0)n(t)\,dV. \tag{5}$$

In Ref. [8], Tomsovic and Heller used the correlation function of the wave function, $\langle\Phi(t=0)|\Phi(t)\rangle$. However, the wave function cannot be measured experimentally. To take advantage of the fact that one can get the density distribution of a BEC in a single measurement with a CCD, we use the evolution of the density correlation C_n to study the role of interatomic interaction.

For the parameters of Fig. 4, before the collision between the matter wave and the corrals, most of the interaction energy has been transferred into kinetic energy. To show more clearly the role of interatomic interaction for stadium-shaped quantum corrals, we consider a different trapping frequency $\omega_\perp = 87.5\pi/10$ (with other parameters being the same as in previous calculations). The purpose of this harmonic trap is to make the size of the condensate comparable to that of the stadium-shaped quantum corrals, so that the interaction energy plays a more important role in the whole process. The inset in Fig. 7 shows the initial density distribution and stadium-shaped quantum corrals for $g_{2D} = 0$. For $g_{2D} = 50$, the interaction energy is about four times the kinetic energy before releasing the harmonic trap, and our calculations show that the interaction energy is comparable to the kinetic energy in the whole dynamic process.

With the parameter $\omega_\perp = 87.5\pi/10$, we show in Fig. 7 the evolution of the density correlation function for different coupling constants. There are two obvious interaction effects: (i) It is shown clearly that, with increasing coupling constant, the density correlation function increases at long-time evolution. This means that increasing the coupling constants has an effect of enhancing the effect of uniform distribution of the matter wave. (ii) We also notice that the oscillation beyond $t = 1$ attenuates more quickly for larger coupling constants. These two interaction effects show that nonlinear interaction can enhance the dynamical quantum chaos.

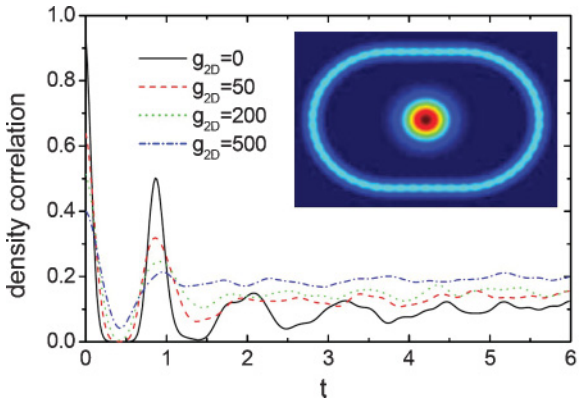

FIG. 7. (Color online) The evolution of the density correlation function for stadium-shaped quantum corrals with different coupling constants. The time t is in units of T_s. The inset displays the initial density distribution and stadium-shaped quantum corrals for $g_{2D} = 0$.

For circle-shaped quantum corrals with the same parameters in Fig. 5, we show in Fig. 8 the density distribution at $t = 6T_c$ for different coupling constants. We see clearly that the density becomes more chaotic as the interaction gets stronger. This indicates that the interaction between atoms can induce quantum chaos at the mean-field level. This interaction-induced chaos is also apparent in the correlation function C_n. Shown in Fig. 9 is the evolution of the density correlation for different coupling constants. As in Fig. 7, we see that the oscillation for long-time evolution attenuates with increasing coupling constants. Without interatomic interaction, the evolution of the density correlation function displays a type of revival oscillation for $t > 3$. For $g_{2D} = 150$ and 500, however, this sort of revival oscillation is not found theoretically. This provides a way to show directly the interaction-induced quantum chaos for the integrable boundary condition.

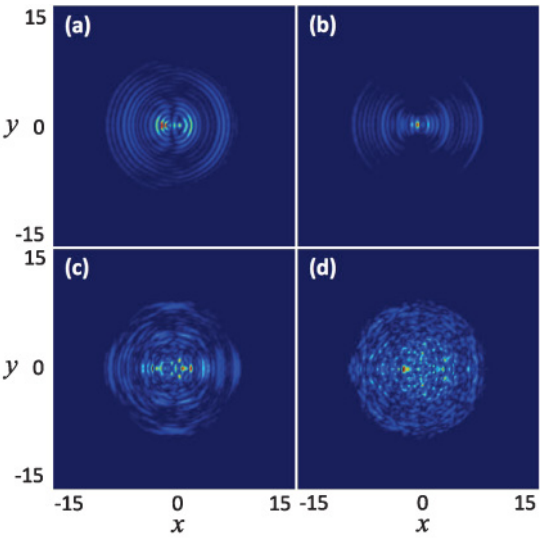

FIG. 8. (Color online) Density distribution at $t = 6T_c$ for circle-shaped quantum corrals with different coupling constants: (a) $g_{2D} = 0$, (b) $g_{2D} = 50$, (c) $g_{2D} = 150$, and (d) $g_{2D} = 500$. The length unit is L_0.

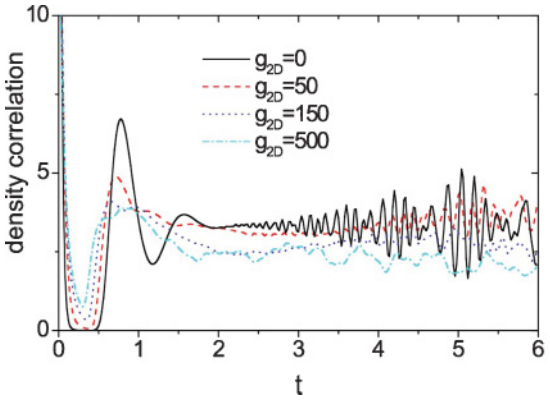

FIG. 9. (Color online) The evolution of the density correlation for circle-shaped quantum corrals with different coupling constants. The time is in units of T_c.

Quantum chaos due to the nonintegrable boundary condition and nonlinear interaction can be understood in the frame of the path integral method,

$$\Phi(x,y,t) = \int K(x,y,t;x_1,y_1,t_1)\Phi(x_1,y_1,t_1)\,dx_1dy_1, \quad (6)$$

where K is a propagator. This propagator is related to the Lagrangian of all possible classical trajectories. So, roughly speaking, for the evolution of a wave packet in quantum corrals, the propagator can be regarded as the supposition of millions of classical trajectories. When the corresponding classical system is integrable, e.g., in circle-shaped corrals, the classical trajectories are regular and lead to a regular wave pattern. When the classical system is chaotic, for example, in stadium-shaped corrals, the classical motion is "random" and chaotic, which, in turn, produces a chaotic-looking density image. Since the interaction in classical mechanics almost always leads to chaotic motion, this implies that interaction can induce quantum chaos, as shown in Fig. 8.

V. SUMMARY AND DISCUSSION

In summary, we have studied an atomic analogy to electronic quantum corrals. A scheme is proposed to study the dynamic evolution of a Bose-Einstein condensate confined in a corral-like potential. In particular, with these atomic corrals, it is now promising to study experimentally the dynamic quantum chaotic behavior [8]. The atomic quantum corrals proposed here can also be applied to study other quantum gases, such as molecular Bose-Einstein condensates [31], degenerate Fermi gases [32], ultracold Fermi gases in the unitarity limit [33], and Bardeen-Cooper-Schrieffer superfluids [34] in the corral-like potential. The different descriptions of the order parameter, quantum statistics, and evolution equation [35] mean that there should be very rich phenomena for discovery.

In the present work, the calculations are carried out with the two-dimensional GP equation. In an experiment, the perpendicular direction may distort the structure in the density distribution shown in our calculations as the density distribution measured by the CCD is an integration along the perpendicular direction. This may be overcome by the method of an optically pumped light sheet, where the absorption of the probe light is restricted to a thin horizontal slice [36].

ACKNOWLEDGMENTS

We acknowledge useful discussions with Baolong Lü, Cheng Chin, Jin Wang, and Li You. This work was supported by NSFC Grant Nos. 10875165, 10825417, and 10634060 and NKBRSF of China Grant No. 2011CB921503.

[1] M. F. Crommie, C. P. Lutz, and D. M. Eigler, Nature (London) **363**, 524 (1993); Science **262**, 218 (1993).
[2] G. A. Fiete and E. J. Heller, Rev. Mod. Phys. **75**, 933 (2003).
[3] G. Colas des Francs, C. Girard, J. C. Weeber, C. Chicane, T. David, A. Dereux, and D. Peyrade, Phys. Rev. Lett. **86**, 4950 (2001).
[4] C. Chicanne, T. David, R. Quidant, J. C. Weeber, Y. Lacroute, E. Bourillot, A. Dereux, G. Colas des Francs, and C. Girard, Phys. Rev. Lett. **88**, 097402 (2002).
[5] K. Southwell, Nature (London) **416**, 205 (2002); J. P. Yin, Phys. Rep. **430**, 1 (2006).
[6] F. Dalfovo, S. Giorgini, L. P. Pitaevskii, and S. Stringari, Rev. Mod. Phys. **71**, 463 (1999); A. J. Leggett, *ibid.* **73**, 307 (2001); C. J. Pethick and H. Smith, *Bose-Einstein Condensation in Dilute Gases* (Cambridge University, Cambridge, 2002); L. P. Pitaevskii and S. Stringari, *Bose-Einstein Condensation* (Clarendon, Oxford, 2003).
[7] E. J. Heller, M. F. Crommie, C. P. Lutz, and D. M. Eigler, Nature (London) **369**, 464 (1994); M. F. Crommie, C. P. Lutz, D. M. Eigler, and E. J. Heller, Phys. D **83**, 98 (1995); Surf. Sci. **361**, 864 (1996).
[8] S. Tomsovic and E. J. Heller, Phys. Rev. Lett. **67**, 664 (1991); Phys. Rev. E **47**, 282 (1993).
[9] S. Tung, V. Schweikhard, and E. A. Cornell, Phys. Rev. Lett. **97**, 240402 (2006).
[10] D. Clement *et al.*, New J. Phys. **8**, 165 (2006).
[11] K. Henderson, C. Ryu, C. MacCormick, and M. G. Boshier, New J. Phys. **11**, 043030 (2009); A. Itah, H. Veksler, O. Lahav, A. Blumkin, C. Moreno, C. Gordon, and J. Steinhauer, Phys. Rev. Lett. **104**, 113001 (2010); V. Boyer, R. M. Godun, G. Smirne, D Cassettari, C. M. Chandrashekar, A. B. Deb, Z. J. Laczik, and C. J. Foot, Phys. Rev. A **73**, 031402(R) (2006).
[12] D. S. Petrov, M. Holzmann, and G. V. Shlyapnikov, Phys. Rev. Lett. **84**, 2551 (2000).
[13] Z. Hadzibabic, P. Krüger, M. Cheneau, B. Battelier, and J. Dalibard, Nature (London) **441**, 1118 (2006); S. Stock, Z. Hadzibabic, B. Battelier, M. Cheneau, and J. Dalibard, Phys. Rev. Lett. **95**, 190403 (2005); P. Kruger, Z. Hadzibabic, and J. Dalibard, *ibid.* **99**, 040402 (2007).
[14] Z. Hadzibabic and J. Dalibard, e-print arXiv:0912.1490.
[15] C.-L. Hung, X. Zhang, N. Gemelke, and C. Chin, Phys. Rev. A. **78**, 011604 (2008).
[16] I. Bloch, J. Dalibard, and W. Zwerger, Rev. Mod. Phys. **80**, 885 (2008).
[17] A. L. Fetter, Rev. Mod. Phys. **81**, 647 (2009); M. R. Matthews, B. P. Anderson, P. C. Haljan, D. S. Hall, C. E. Wieman, and

E. A. Cornell, Phys. Rev. Lett. **83**, 2498 (1999); K. W. Madison, F. Chevy, W. Wohlleben, and J. Dalibard, *ibid.* **84**, 806 (2000); J. R. Abo-Shaeer, C. Raman, J. M. Vogels, and W. Ketterle, Science **292**, 476 (2001); P. C. Haljan, I. Coddington, P. Engels, and E. A. Cornell, Phys. Rev. Lett. **87**, 210403 (2001); M. F. Andersen, C. Ryu, P. Clade, V. Natarajan, A. Vaziri, K. Helmerson, and W. D. Phillips, *ibid.* **97**, 170406 (2006); D. R. Scherer, C. N. Weiler, T. W. Neely, and B. P. Anderson, *ibid.* **98**, 110402 (2007); E. A. L. Henn, J. A. Seman, G. Roati, K. M. F. Magalhães, and V. S. Bagnato, *ibid.* **103**, 045301 (2009); C. N. Weiler *et al.*, Nature (London) **455**, 948 (2008); Y.-J. Lin *et al.*, *ibid.* **462**, 628 (2009).

[18] C. W. Zhang, J. Liu, M. G. Raizen, and Q. Niu, Phys. Rev. Lett. **93**, 074101 (2004).

[19] W. Hai, S. Rong, and Q. Zhu, Phys. Rev. E **78**, 066214 (2008); W. Hai, Q. Zhu, and S. Rong, Phys. Rev. A **79**, 023603 (2009); Q. Zhu, W. Hai, and S. Rong, Phys. Rev. E **80**, 016203 (2009).

[20] N. Katz and O. Agam, New J. Phys. **12**, 073020 (2010).

[21] D. A. Steck, W. H. Oskay, and M. G. Raizen, Science **293**, 274 (2001).

[22] V. Milner, J. L. Hanssen, W. C. Campbell, and M. G. Raizen, Phys. Rev. Lett. **86**, 1514 (2001).

[23] N. Friedman, A. Kaplan, D. Carasso, and N. Davidson, Phys. Rev. Lett. **86**, 1518 (2001).

[24] M. F. Andersen, A. Kaplan, T. Grűnzweig, and N. Davidson, Phys. Rev. Lett. **97**, 104102 (2006).

[25] T. A. Pasquini, Y. Shin, C. Sanner, M. Saba, A. Schirotzek, D. E. Pritchard, and W. Ketterle, Phys. Rev. Lett. **93**, 223201 (2004).

[26] N. Gemelke, X. B. Zhang, C. L. Hung, and C. Chin, Nature (London) **460**, 995 (2009); W. S. Bakr, J. I. Gillen, A. Peng, S. Folling, and M. Greiner, *ibid.* **462**, 74 (2009); W. S. Bakr *et al.*, Science **329**, 547 (2010); J. F. Sherson *et al.*, Nature (London) **467**, 68 (2010).

[27] H. J. Stöckmann, *Quantum Chaos: An Introduction* (Cambridge University, Cambridge, 1999).

[28] J. Stein, H. J. Stöckmann, and U. Stoffregen, Phys. Rev. Lett. **75**, 53 (1995).

[29] M. R. Andrews *et al.*, Science **275**, 637 (1997).

[30] C. Chin, R. Grimm, P. Julienne, and E. Tiesinga, Rev. Mod. Phys. **82**, 1225 (2010).

[31] S. Jochim *et al.*, Science **302**, 2101 (2003); M. Greiner, C. A. Regal, and D. S. Jin, Nature (London) **426**, 537 (2003); M. W. Zwierlein, C. A. Stan, C. H. Schunck, S. M. F. Raupach, S. Gupta, Z. Hadzibabic, and W. Ketterle, Phys. Rev. Lett. **91**, 250401 (2003).

[32] B. D. Marco and D. S. Jin, Science **285**, 1703 (1999).

[33] K. M. O'Hara *et al.*, Science **298**, 2179 (2002).

[34] C. A. Regal, M. Greiner, and D. S. Jin, Phys. Rev. Lett. **92**, 040403 (2004); M. W. Zwierlein, C. A. Stan, C. H. Schunck, S. M. F. Raupach, A. J. Kerman, and W. Ketterle, *ibid.* **92**, 120403 (2004); M. Bartenstein, A. Altmeyer, S. Riedl, S. Jochim, C. Chin, J. H. Denschlag, and R. Grimm, *ibid.* **92**, 120401 (2004); J. Kinast, S. L. Hemmer, M. E. Gehm, A. Turlapov, and J. E. Thomas, *ibid.* **92**, 150402 (2004).

[35] S. Giorgini, L. P. Pitaevskii, and S. Stringari, Rev. Mod. Phys. **80**, 1215 (2008).

[36] S. Inouye, S. Gupta, T. Rosenband, A. P. Chikkatur, A. Görlitz, T. L. Gustavson, A. E. Leanhardt, D. E. Pritchard, and W. Ketterle, Phys. Rev. Lett. **87**, 080402 (2001).